

Article

Synergy of Road Network Planning Indices on Central Retail District Pedestrian Evacuation Efficiency

Gen Yang ¹, Tiejun Zhou ^{1,*}, Mingxi Peng ², Zhigang Wang ² and Dachuan Wang ³

¹ School of Architecture and Urban Planning, Chongqing University, Chongqing 400045, China

² The Department of Smart Urban Design, Chongqing Jianzhu College, Chongqing 400072, China

³ School of Civil Engineering and Architecture, Southwest University of Science and Technology, Mianyang 621010, China

* Correspondence: 20151502021@cqu.edu.cn; Tel.: +86-157-2341-0933

Abstract: Pedestrian evacuation is an important measure to ensure disaster safety in central retail districts, the efficiency of which is affected by the synergy of road network planning indices. This paper established the typical forms of central retail district (CRD) road networks in terms of block form, network structure and road grade, taking China as an example. The experiment was designed using the orthogonal design of experiment (ODOE) method and quantified the evacuation time under different road network planning indices levels through the Anylogic simulation platform. Using range and variance analysis methods, the synergy of network density, network connectivity, road type and road width on pedestrian evacuation efficiency were studied from the perspectives of significance, importance and optimal level. The results showed that the type of CRD will affect the importance of network planning indices, and that the network connectivity is insignificant ($P = 0.477/0.581$) in synergy; networks with wide pedestrian primary roads (30.1~40.0 m), medium secondary roads (3.1~5.0 m/side) and high density (11.0~13.0 km/km²) have the highest evacuation efficiency. From the perspective of evacuees, this paper put forward urban design implications on CRD road networks to improve their capacity for disaster prevention and reduction.

Keywords: central retail district (CRD); road network planning; pedestrian evacuation efficiency; synergy; urban design



Citation: Yang, G.; Zhou, T.; Peng, M.; Wang, Z.; Wang, D. Synergy of Road Network Planning Indices on Central Retail District Pedestrian Evacuation Efficiency. *ISPRS Int. J. Geo-Inf.* **2023**, *12*, 239. <https://doi.org/10.3390/ijgi12060239>

Academic Editors: Maria Antonia Brovelli, Songnian Li and Wolfgang Kainz

Received: 28 March 2023

Revised: 3 June 2023

Accepted: 7 June 2023

Published: 9 June 2023



Copyright: © 2023 by the authors. Licensee MDPI, Basel, Switzerland. This article is an open access article distributed under the terms and conditions of the Creative Commons Attribution (CC BY) license (<https://creativecommons.org/licenses/by/4.0/>).

1. Introduction

In the 21st century, urban safety is facing a more complicated and urgent situation [1,2]. Due to the dense structure, central geographical location, complex functional attributes, and three-dimensional traffic organization, CRDs are fragile systems with high disaster-sensitivity [3,4]. The potential threat caused by various emergencies is serious, which makes CRDs become the focus of urban disaster prevention and evacuation research. Facing devastating disasters such as earthquakes, explosions, toxic gas and terrorist attacks, pedestrian evacuation is not only the first reaction of evacuees, but also the most effective evacuation mode in high density urban areas (population density exceeds 100,000 p/km²) such as CRDs [5,6]. For example, in the explosion in Tianjin Binhai New Area in 2015, residents within 3 km spontaneously or were guided to evacuate on foot. As the environmental foundation of pedestrian evacuation, urban road network planning indices affect the evacuation efficiency [7–11]. Additionally, systematic research on it has become a prerequisite to ensure urban safety and achieve sustainable urban development. However, the 406 million vehicles in China [12] mean that CRD road network planning and construction still takes “car standard” as the primary objective. In specialized urban disaster prevention and evacuation research, the question of how to formulate CRD road network construction suggestions for evacuees and improve the efficiency of pedestrian evacuation are urgent problems to be solved.

In urban evacuation, the pedestrian evacuation road network has experienced a development from macroscopic qualitative research to meso-microscopic quantitative research. These disciplines include urban planning [13–16], transportation [17–19] and urban design [20–22]. Relevant conclusions discuss the interaction between evacuation environments and evacuees. Urban road networks are the spatial carrier of pedestrian evacuation, thus affecting the efficiency of pedestrian evacuation directly. The main planning indices that determine the form of urban road network include three levels: block form, network structure and road grade. For example, Shi et al. (2020) [23] chose block area and block elongation as indices and quantified the road network patterns of five high density blocks in Singapore. Using Open Street Map (OSM) data, Minaei (2020) [24] analyzed the changes in density and connectivity of road network morphology in major cities in Iran. Jiang (2022) [25] took Dartford, Kent County, UK, as the research object and emphasized the influence of road width and road type on the urban road network form. In addition, [26] pointed out that the CRD transportation and distribution relationship is special, and the planning indices of primary and secondary road networks should be studied separately.

Currently, the relevant research mainly analyzes the influence of single road network planning indices on pedestrian evacuation efficiency. Based on the case of Shanghai, Jin et al. (2021) [27] discussed the influence of road type on the pedestrian evacuation efficiency of the underground city road network by using the formulated network flow model. Zuo et al. (2021) [22] verified the effect of road width on pedestrian evacuation efficiency in the Jintang Road area of Tianjin using agent-based modeling (ABM) simulation technology. Irsyad et al. (2022) [28] simulated the evacuation situation of evacuees in Kampongs, Yogyakarta, Indonesia, through spatial syntax and analyzed the influence of network structure indices such as network connectivity on the pedestrian evacuation efficiency. However, a CRD road network is a complex system affected by multiple indices. The efficiency of pedestrian evacuation is the synergy result of several indices [29]. It is not objective for one single planning indices to explain the results of pedestrian evacuation. Nor can it reflect the specific impact of different indices in synergy. The factorial design of experiment (FDOE) [30] research method, based on multi-factor synergy, can explore the relationship between independent-dependent variables and can also reveal the relationship among independent variables. However, its application in the research of CRD pedestrian evacuation is insufficient.

Evacuation time is an important index in quantifying pedestrian evacuation efficiency [31,32]. The main quantitative methods can be divided into two categories at present: mathematical models and computer simulations [33]. Among them, mathematical models regard pedestrian evacuation as a static/dynamic path selection problem. They usually takes the shortest evacuation time, the smallest overall delay, the shortest evacuation path and the largest traffic capacity [15,19,34] as the research objectives to guide the planning and design of road networks. Mathematical models ignore the behavior characteristics of evacuees and the interaction between evacuees and their environment. Pedestrian evacuation planning is a dynamic network-flow problem with a time process. The optimal solution in mathematical modeling may not be applicable the real situation. With the development of computer technology, agent-based modeling (ABM) simulation technology can realistically reflect the complex interaction between evacuees and environment. Additionally, it has received widespread attention in the refined and quantitative research of pedestrian evacuation [35–38].

Establishing urban road network models is the basis of using ABM simulation platforms to predict/restore pedestrian evacuation scenarios. Cheng et al. (2020) [39] took ‘Olympic Park Station’ in Beijing as an experimental case and used an ABM simulation platform to study the evacuation risk of underground roads. Zuo et al. (2021) [22] analyzed the influence of road network indices on pedestrian evacuation efficiency by using the Anylogic platform, taking the Jintang Road area in Tianjin as the research object. This kind of simulation research based on specific cases can solve the problems of one single object, but the research conclusions are not universal. Moreover, because the modeling of

specific cases involves the restoration of the evacuation environment, the research results are influenced by irrelevant factors. As such, the typical model research method [40–43] based on typology is more suitable in discussing CRD pedestrian evacuation problems. It can effectively eliminate the interference caused by redundant factors and enhance the application significance of research results. However, the research results on the typical model of CRD road networks are relatively insufficient.

This study is an extension of the existing research results and innovatively analyzes the synergy of multiple road network planning indices on CRD pedestrian evacuation efficiency. The typical forms of CRD road network under different transportation and distribution are extracted from three levels: block form, network structure and road grade. By using the ABM simulation method and FDOE analysis method, the synergy of road network planning indices on pedestrian evacuation efficiency will be quantified. The CRD road network optimization policy and strategy for optimizing pedestrian evacuation efficiency are put forward from the perspective of evacuees. The remainder of the paper is organized as follows: the study materials, experiment setup and methods involved in this paper are elaborated in Section 2. Section 3 presents the experimental results. The discussion and conclusion are described in Sections 4 and 5 separately.

This study is also a part of the National Natural Science Foundation of China (NSFC) projects “Urban Central Business District Open Space Design for Pedestrian Evacuation Response to Emergency Events” and “Research on Design of Deep Underground Space Multi-level Evacuation Network Guided by Sub-safety Area”. From 2017 to 2022, the map information and location-based Service (LBS) data of CRDs in China were investigated, and the relevant research results will also be used in this study.

2. Methods

The methodological framework of this study is presented in the following steps (Figure 1):

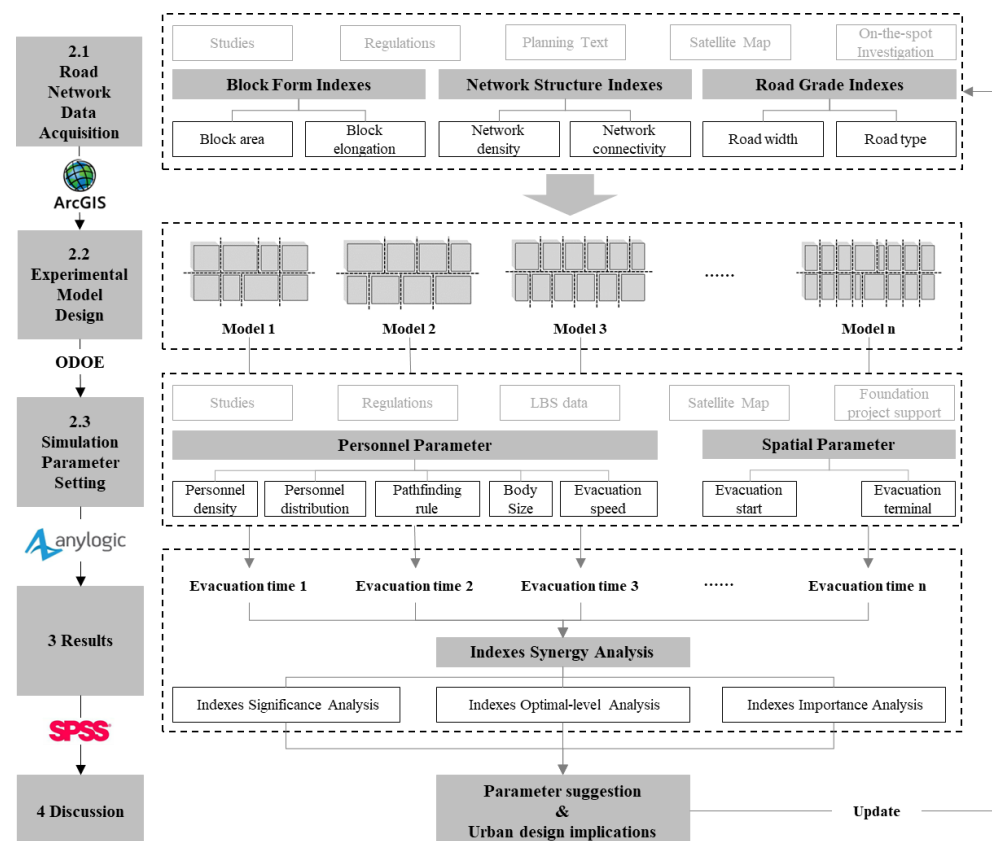


Figure 1. Research workflow and the tools used.

Acquire the road network data from three levels: block form, network structure and road grade, based on the surveys of CRD samples in China. Establish the range of road network planning indices and typical CRD road network forms, providing basic data for research.

Determine the planning indices levels of CRD road networks according to the ODOE analysis method based on factor synergy, providing the variable parameters of the ABM simulation test.

Use the ABM simulation platform to research the synergy of network density, network connectivity, road width and road type on pedestrian evacuation efficiency at different levels, providing theoretical support for CRD road network optimization suggestions.

Propose the implications for optimizing the guidelines and strategies of CRD road networks of the above results.

2.1. Road Network Data Acquisition

2.1.1. Study Area Selection

The CRDs of the top six cities in China's comprehensive business index (Beijing, Shanghai, Guangzhou, Shenzhen, Chengdu and Chongqing) [44] were selected as exemplary areas in Figure 2. Excluding the similar samples of central business districts (CBD), recreational business districts (RBD) and urban complexes, nine CRDs at city level were selected as the research objects. These objects are of strip and mesh CRD types, which have obvious typological characteristics for transportation and distribution [26].

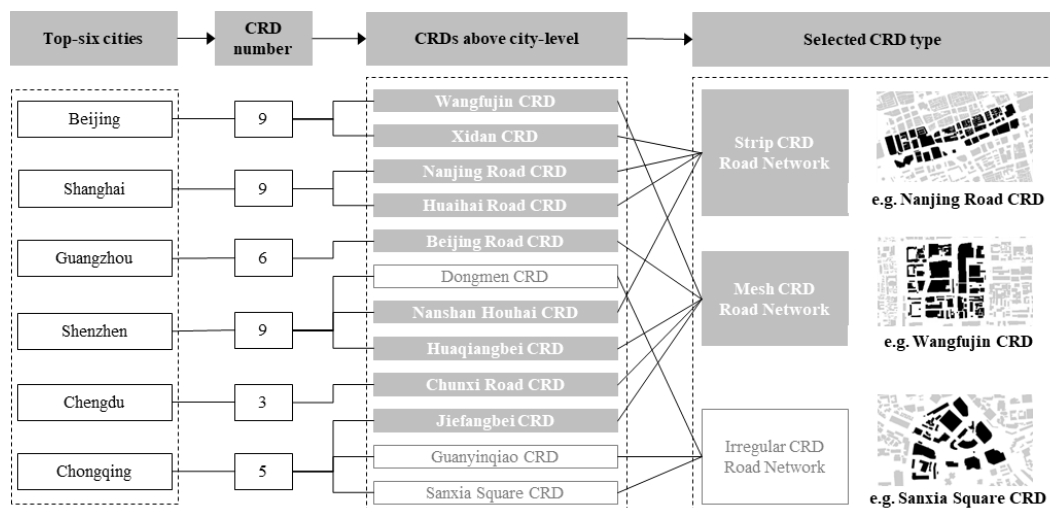


Figure 2. The nine selected CRDs' distribution and type.

2.1.2. Road Network Planning Indices Selection

In urban design, figure-ground theory [45] points out that the composition mode of "block" and "road" leads to the particularity in "network". The three factors jointly determine the CRD road network form and affect the efficiency of pedestrian evacuation. Therefore, based on the relevant literature studies and design regulations, this paper puts forward six road network planning indices: block area, block elongation, network density, network connectivity, road type and road width, from three aspects: "block form", "road grade" and "network structure" (Figure 3). Refer to Table 1 for details of quantification methods. Block form indices were divided into "inner block" and "entire block" in order to guarantee the authenticity of the typical model. Similarly, the road grade indices were divided into "primary road" and "secondary road". This study used the ArcGIS platform to process CRD road network indices data, which was acquired from the open resources of Baidu satellite map data, regulatory planning documents and commercial network development planning documents.

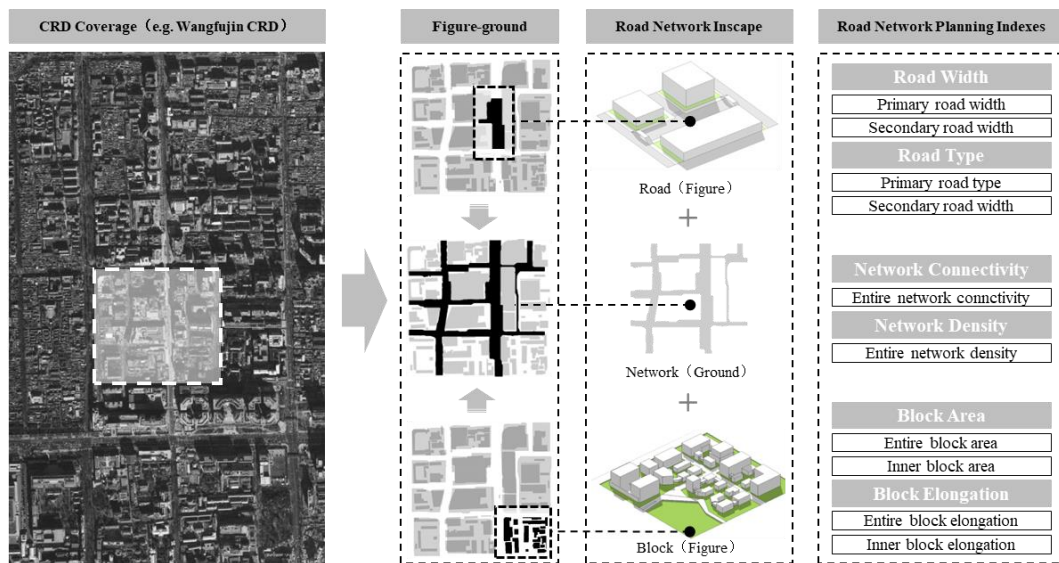


Figure 3. The road network figure-ground relationship and planning indices.

Table 1. Summary of road network planning indices.

Index	Formula	Unit	Explaining
block area [23]	-	km ²	The size of a block.
block elongation (<i>ELG</i>) [23]	$ELG = \frac{D_1}{D_2}$	-	The geometry of a block. D_1 is the equivalent circle diameter with the same area as the block; D_2 is the minimum circumscribed diameter of the block. The closer the value is to 0.80, the closer the shape is to square. <i>ELG</i> is often expressed in terms of length-width ratio.
network density (<i>D</i>) [46]	$D = \frac{L}{S}$	km/km ²	The rationality of a road network. <i>L</i> is the road length; <i>S</i> is the size of area. <i>D</i> in this study is the density of all roads. The rationality should be discussed according to traffic demand.
network connectivity (<i>J</i>) [47]	$J = \frac{2M}{N}$	-	The development level of a road network. <i>N</i> is the road node number; <i>M</i> is the number of road sections. <i>J</i> in this study is the connectivity of all roads. The higher the value, the higher the road network development level.
road type [48]	-	-	The section composition of roads. CRD road mainly include two types: pedestrian traffic and mixed traffic with a pedestrian section on both sides.
road width (<i>W</i>) [48]	$W = 3.5n + W_p$	m	The width of all road sections. <i>n</i> is the number of motor vehicle sections, the width of which is limited to 3.5 m/lane; W_p is the pedestrian section width. Each road width should be the minimum width due to the buckets-effect.

2.1.3. Typical CRD Road Network Form

This research investigated road network planning indices data of 53 roads and 98 blocks in nine CRDs. Two types of typical CRD road network forms were put forward from three aspects: block form, network structure and road grade.

1. Block form

In order to reflect the difference of parameters, this paper established two typical CRD block forms with low elongation (A-type: mesh CRD, length-width ratio 1:1) and high elongation (B-type: strip CRD, length-width ratio 2:1). The typical block area is based on

the truncated mean value of 0.25 km² (standard deviation 0.02) to ensure the comparability of the research results. To eliminate the interference caused by the disorderly combination of inner blocks, this paper used three standard length–width ratios (2:2, 3:2 and 4:2). The typical inner block area is 0.05 km, and the length range of each side is 0.05~0.20 km (the fluctuation range of ±0.02 km is reserved). See Figure 4 for details.

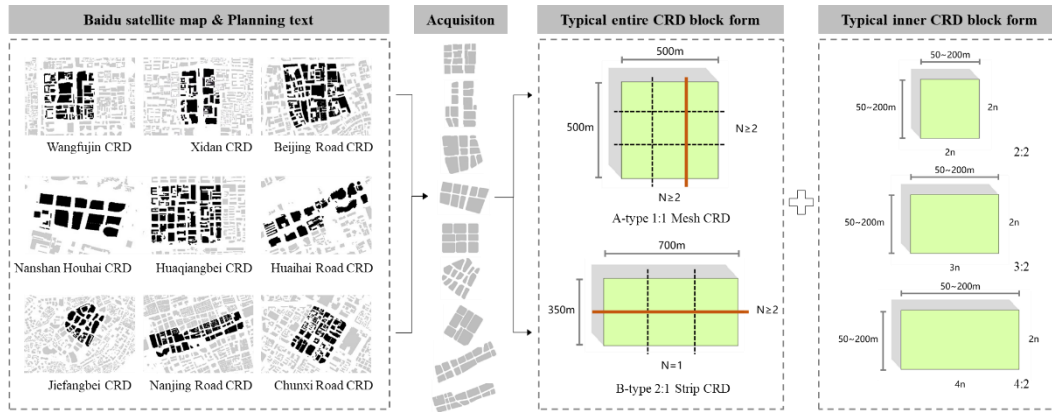


Figure 4. The typical block forms of two CRD types.

2. Network structure

According to the survey results, 5.1~8.0 km/km², 8.1~10.0 km/km² and 10.1~13.0 km/km² were set as “low density”, “medium density” and “high density” ranges. Similarly, 4.0~4.6, 4.7~5.3 and 5.4~6.0 were set as “low connectivity”, “medium connectivity” and “high connectivity” ranges. Under the condition of smooth primary roads, the typical CRD network structure was set up with the typical CRD block form as the basic unit. This research put forward 18 types of network structure under two CRD types, which included 3 kinds of network density and 3 kinds of network connectivity. The specific expressions are shown in Table 2.

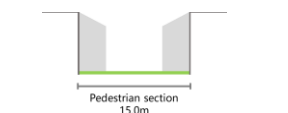
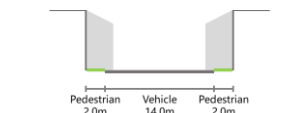
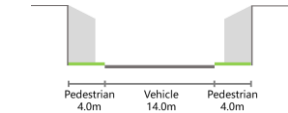
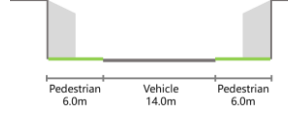
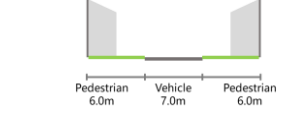
Table 2. The typical network structure of two CRD types.

	Mesh CRD Type			Strip CRD Type		
	Low Density 8.0 km/km ²	Medium Density 10.0 km/km ²	High Density 12.0 km/km ²	Low Density 7.0 km/km ²	Medium Density 9.8 km/km ²	High Density 12.6 km/km ²
high connectivity (5.4~6.0)	Aa1	Ab1	Ac1	Ba1	Bb1	Bc1
medium connectivity (4.7~5.1)	Aa2	Ab2	Ac2	Ba2	Bb2	Bc2
low connectivity (4.0~4.5)	Aa3	Ab3	Ac3	Ba3	Bb3	Bc3

3. Road grade

The survey results showed that primary roads include two types: pedestrian-traffic roads and mixed-traffic roads, and the secondary roads are mainly mixed-traffic roads. The vehicle section width of the primary road and secondary road was set as four lanes (100% in the survey result) and two lanes (69.1% in the survey result), respectively. The “narrow width”, “medium width” and “broad width” ranges of primary road pedestrian section were 10.1~20.0 m, 20.1~30.0 m and 30.1~40.0 m, and the secondary road were 1.1~3.0 m, 3.1~5.0 m and 5.1~7.0 m. The standard width of each road was set as the median value of survey result: 15 m, 25 m and 35 m for the pedestrian-traffic road and 2 m, 4 m and 6 m for the pedestrian section in the mixed-traffic road. Refer to Table 3 for setting details.

Table 3. The typical road grade of CRD road network.

	Primary Road		Secondary Road
	Pedestrian-Traffic Road	Mixed-Traffic Road	Mixed-Traffic Road
narrow width	 Pedestrian section 15.0m P1 (15 m)	 Pedestrian 2.0m Vehicle 14.0m Pedestrian 2.0m M11 (2 × 2 m + 14 m)	 Pedestrian 2.0m Vehicle 7.0m Pedestrian 2.0m M21 (2 × 2 m + 7 m)
medium width	 Pedestrian section 25.0m P2 (25 m)	 Pedestrian 4.0m Vehicle 14.0m Pedestrian 4.0m M12 (2 × 4 m + 14 m)	 Pedestrian 4.0m Vehicle 7.0m Pedestrian 4.0m M22 (2 × 4 m + 7 m)
broad width	 Pedestrian section 35.0m P3 (35 m)	 Pedestrian 6.0m Vehicle 14.0m Pedestrian 6.0m M13 (2 × 6 m + 14 m)	 Pedestrian 6.0m Vehicle 7.0m Pedestrian 6.0m M23 (2 × 6 m + 7 m)

2.2. Experimental Model Design

Orthogonal design of experiments (ODOE) [49] is a branch of FDOE, which can obtain test results from a few original experiments. Unlike some other traditional research methods, it can weight all non-numerical comparisons using statistical calculation. Based on a suitable orthogonal test table, representative cases with uniform dispersion, neatness and comparability can be selected from the original test. Testing these cases can simplify the research process. ODOE has been applied to many disciplines because of its comprehensive, efficient and controllable advantages.

The block form is the spatial expression of the basic units of the CRD road network simulation test model. However, the multi-level indices are the direct factors affecting the pedestrian evacuation efficiency. Therefore, the network structure and road grade-related indices were set as experimental variables referring to the typical CRD road network form. The primary road width (A), secondary road width (B), network density (C), network connectivity (D) and primary road type (E) were included. Refer to Table 4 for the experimental level setting of each variable. This research used the ODOE method to optimize the simulation test scheme in order to simplify the 162 simulations of the comprehensive test. According to the number of variables and levels, the orthogonal test standard table L_{18} (2×3^7) was selected. With the combination–method columns adjustment, 18 test schemes were obtained; that is, only 18 representative conditions need to be simulated.

Table 4. ODOE experimental variables and levels setting.

CRD Type	Levels	Primary Road Width (A)	Secondary Road Width (B)	Network Density (C)	Network Connectivity (D)	Primary Road Type (E)
strip CRD	1	15 m/2 × 2 + 14 m	2 × 2 + 7 m	7 km/km ²	4.0~4.5	pedestrian traffic
	2	25 m/4 × 2 + 14 m	4 × 2 + 7 m	9.8 km/km ²	4.7~5.1	mixed traffic
	3	35 m/6 × 2 + 14 m	6 × 2 + 7 m	12.6 km/km ²	5.4~6.0	-
mesh CRD	1	15 m/2 × 2 + 14 m	2 × 2 + 7 m	8 km/km ²	4.0~4.5	pedestrian traffic
	2	25 m/4 × 2 + 14 m	4 × 2 + 7 m	10 km/km ²	4.7~5.1	mixed traffic
	3	35 m/6 × 2 + 14 m	6 × 2 + 7 m	12 km/km ²	5.4~6.0	-

2.3. Simulation Parameter Setting

The ABM platform currently supporting pedestrian flow simulation includes Anylogic, Simulex, STEPS, Building EXODUS, etc. Among them, Anylogic platform based on the social force model [50] can excellently restore the discrete and continuous interaction between evacuees and the evacuation environment by using multi-agent technology. In the Anylogic pedestrian flow model, the human agents will be affected by three types of forces during the travel: the driving forces from pedestrians’ subjective wills; the repulsive force between pedestrians and the environment; the social forces between pedestrians, which maintain each other at a certain distance. These forces can be described by the following formula:

$$\vec{f}_\alpha(t) = \vec{f}_\alpha^0(\vec{v}_\alpha) + \vec{f}_{\alpha B}(\vec{r}_\alpha) + \sum_{\beta(\neq\alpha)} \vec{f}_{\alpha\beta}(\vec{r}_\alpha, \vec{v}_\alpha, \vec{r}_\beta, \vec{v}_\beta) + \sum_{\beta(\neq\alpha)} \vec{f}_{\alpha i}(\vec{r}_\alpha, \vec{r}_i, t) \quad (1)$$

$\vec{f}_\alpha^0(\vec{v}_\alpha)$ is an accelerated force. $\vec{f}_{\alpha B}(\vec{r}_\alpha)$ is the force between human agents and boundaries/obstacles. $\vec{f}_{\alpha\beta}(\vec{r}_\alpha, \vec{v}_\alpha, \vec{r}_\beta, \vec{v}_\beta)$ and $\vec{f}_{\alpha i}(\vec{r}_\alpha, \vec{r}_i, t)$ are the forces between different human agent α and β . These forces will drive pedestrians to act in certain behaviors and paths, which are calculated in Anylogic based on Dijkstra’s algorithm, and can be called through Java language coding. Anylogic can simulate the evacuation process by setting different personnel and spatial parameters of the evacuees and evacuation environments (Figure 5). With the visualization characteristics and real-time data, it is convenient for calculating evacuation time and analyzing the cause of congestion. In addition, it is the first software platform to use the UML language to simulate the mixed state of a people flow system. Therefore, Anylogic is more computationally expensive than qualitative spatial analysis methods, but more accurate and scientifically valid [51].

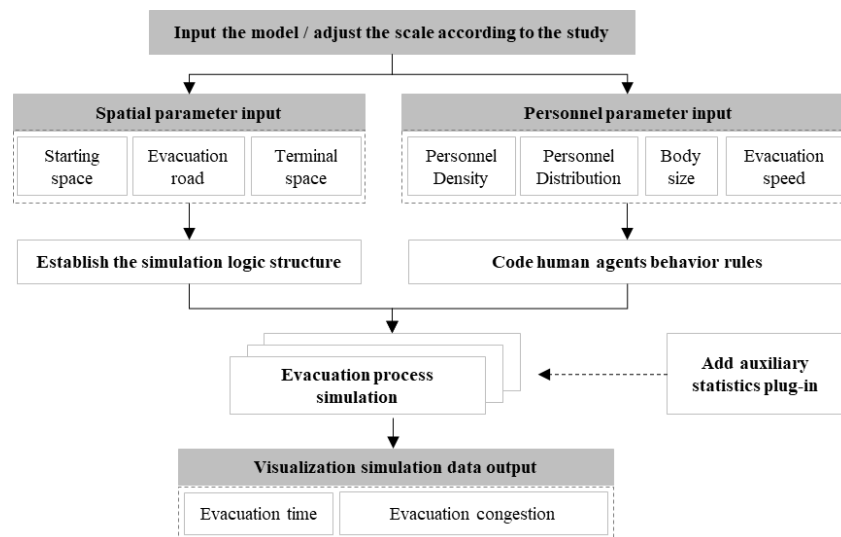


Figure 5. Anylogic simulation process design.

This study was based on Anylogic platform, which has good adaptability to the analysis of CRDs' road network [21], and the simulation results can truly restore the real-world evacuation scene [52,53]. The data of simulation parameter setting is supported by the projects of NSFC. These data were derived from the 9 typical CRDs selected in Section 2.1, which divided into two categories: the LBS data provided by Baidu thermal map; the satellite map data provided by DigitalGlobe. The survey was conducted at 8:00~22:00 on 11 January (Tuesday)/15 (Saturday) in 2022, and 144 valid data were extracted by ArcGIS. The setting of simulation parameter was also influenced by relevant codes and literatures, specific as follows.

2.3.1. Personnel Parameter Setting

1. Personnel density

The CRD personnel density was set according to average Baidu thermal map data on a weekday and rest day (11 and 15 January 2022). The statistical results of the daily average personnel density in 9 CRD samples are shown in Table 5. In order to make the research results more universal, the standard parameter of medium density of 0.3 people/m² is selected as the simulation parameter.

Table 5. CRD personnel density according to Baidu thermal map.

Level	Range	Average	Standard
low density	0.08~0.15 p/m ²	0.13 p/m ²	0.1 p/m ²
medium density	0.20~0.45 p/m ²	0.32 p/m ²	0.3 p/m ²
high density	0.29~0.55 p/m ²	0.48 p/m ²	0.5 p/m ²

2. Personnel distribution

The personnel distribution shows obvious differences due to distinct forms of CRD transportation and distribution. According to the visual LBS data from Baidu thermal maps on a weekday and rest day (11 and 15 January 2022), it was found that people show the characteristics of central gathering and axial extension in the mesh CRD and strip CRDs, respectively. The entire CRD area was divided into equal parts in the setting process, and the number of people in each part was reduced step by step according to the distribution characteristics. Details were shown in Figure 6.

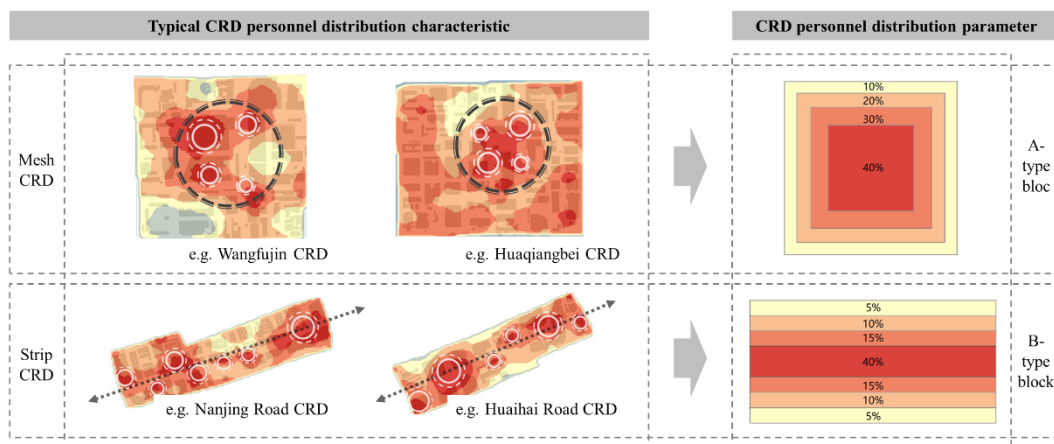


Figure 6. CRD personnel distribution and parameter setting.

3. Pathfinding rule

The behavior with the purpose of escape will prompt people to choose the shortest path to evacuate in emergency situations [54]. Additionally, in order to ensure the safety and effectiveness of pedestrian evacuation, it is usually recommended to evacuate with

ground facilities [7]. Therefore, the pedestrian in our simulation test was set up to select the nearest exit according to the guidance sign and use the ground facilities to evacuate. Since motor vehicle traffic in the regulated and unregulated state is not safe for pedestrian evacuation [55], the simulation test set the pedestrian sections of the road as the evacuation space. Additionally, the safety islands were always in a passable state during the evacuation process.

4. Body size

In the Anylogic platform, the body size of evacuees is treated as a cylindrical shape, and the radius of agents is mainly affected by the shoulder width. According to the Chinese Adult Body Size (GB/T 10000-1988) (Table 6), the median shoulder width of adults was 0.43 m (male) and 0.4 m (female); we used this as the standard simulation parameter, accounting for 40% and 60%, respectively [56].

Table 6. Maximum shoulder width of human body(mm).

Male (Age: 18~60)	383	398	405	431	460	469	486
Female (Age: 18~55)	347	363	371	397	428	438	458
Percentile	1	5	10	50	90	95	99

5. Evacuation speed

The evacuation speed, set according to the young and middle-aged people, who are the main population of CRDs [56], in the non-crowded state is 1.4 m/s. When congestion occurs, the evacuation speed was simulated using the Anylogic platform to obtain the attenuation change under different crowd densities; when the crowd density exceeds 4.1 p/m², the evacuation speed was considered to be 0 m/s [57], and the crowd was at a standstill.

2.3.2. Spatial Parameter Setting

1. Evacuation starting space

In the study of evacuation in urban design, the starting space is considered as the transition interface between different regions. Based on the typical forms of CRD road network, the interfaces between different blocks and roads were set as the initial outflow interface of evacuees. The specific outflow (n , p/m/s) was calculated using the following formula.

$$n = A_{GF} \times \rho_{GF} \times D_{GF} \times N/100 \quad (2)$$

In the formula: A_{GF} is the ground floor area of commercial buildings within the block, calculated with 50% occupation rate according to the local land planning regulations; ρ_{GF} is the density of people on the commercial buildings' ground floor, taking 0.5 people/m² as the standard value with reference to *Regulation for Design of Stores (JGJ48-2014)*; D_{GF} is the minimum evacuation exit width for 100 people, which is 0.65 m/100 p according to *Regulation for Fire Protection Design of Buildings (GB 50016-2014, 2018 edition)*; N is the flow rate, for which 1 p/m/s was taken as the standard. In the simulation process, people were generated randomly from the four sides of each block.

2. Evacuation terminal space

Due to the severe shortage of open space in CRDs [4], the proportion of emergency shelters construction barely meets the evacuation demand (Figure 7). This means it is necessary to coordinate the surrounding urban space for evacuation. In the setting of an evacuation terminal, it was considered that the evacuation is completed when the evacuees arrive at the boundary road of CRD simulation model, and the Ped-sink command was used to avoid the road network node congestion from affecting the test results.

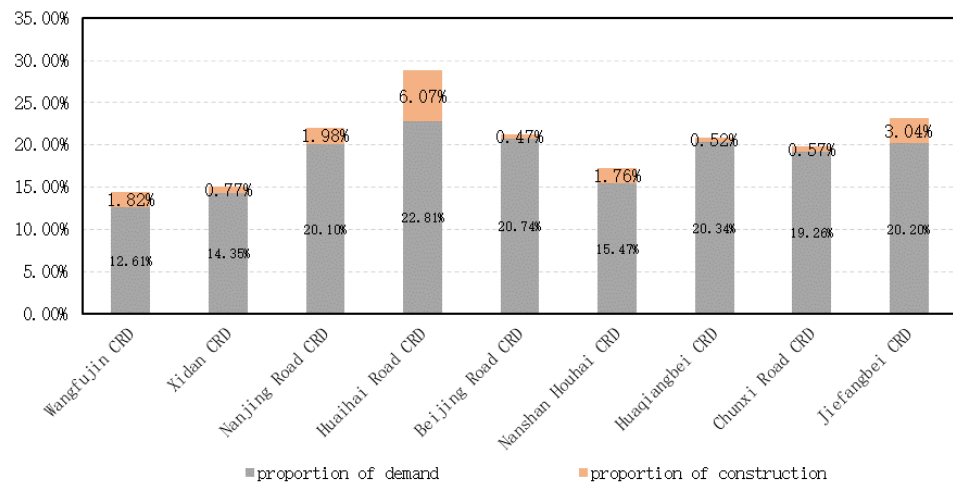


Figure 7. The proportion of emergency shelters in CRDs.

3. Results

The research used the simulation results as the basic data for analyzing the synergy of multiple indices (Table 7). In order to reduce the deviation of the simulation, the point at which 85% of the people had completed the evacuation was selected as the evaluation standard of the pedestrian evacuation efficiency. Additionally, the entirety attenuation average level of the personnel density in the road network was used to assist the discussion of the research results. Based on the conclusion analysis of the orthogonal test, the significance, importance and optimal level of each index in the synergy were explored by using the variance method and range method.

Table 7. ODOE standard table $L_{18} (2 \times 3^7)$ with adjustment and simulation result.

Test ID	Index-Level					Simulation Test Model ID		Evacuate Time (85%) (s)	
	Index A	Index B	Index C	Index D	Index E	Strip CRD	Mesh CRD	Strip CRD	Mesh CRD
1	1	1	2	2	1	P1M21Bb2	P1M21Ab2	535	580
2	1	2	3	3	1	P1M22Bc3	P1M22Ac3	365	400
3	1	3	1	2	1	P1M23Ba2	P1M23Aa2	410	585
4	2	1	2	3	1	P2M21Bb3	P2M21Ab3	460	560
5	2	2	3	1	1	P2M22Bc1	P2M22Ac1	305	385
6	2	3	1	3	1	P2M23Ba3	P2M23Aa3	435	555
7	3	1	2	1	1	P3M21Bb1	P3M21Ab1	340	465
8	3	2	3	2	1	P3M22Bc2	P3M22Ac2	285	370
9	3	3	1	3	1	P3M23Ba3	P3M23Aa3	410	555
10	1	1	3	3	2	M11M21Bc3	M11M21Ac3	530	685
11	1	2	1	1	2	M11M22Ba1	M11M22Aa1	590	720
12	1	3	2	2	2	M11M23Bb2	M11M23Ab2	510	615
13	2	1	2	3	2	M12M21Bb3	M12M21Ab3	580	720
14	2	2	3	1	2	M12M22Bc1	M12M22Ac1	395	535
15	2	3	1	2	2	M12M23Ba2	M12M23Aa2	465	620
16	3	1	3	2	2	M13M21Bc2	M13M21Ac2	460	580
17	3	2	1	3	2	M13M22Ba3	M13M22Aa3	445	610
18	3	3	2	1	2	M13M23Bb1	M13M23Ab1	380	515

3.1. Indices Significance Analysis

The significance analysis based on the variance method was used to test whether the road network indicators are associated with pedestrian evacuation efficiency under the synergistic effect. The test results of the two CRD types were shown in Table 8: the R^2 values were 0.900 and 0.943, respectively, indicating that indices A~E have a very significant impact on CRD pedestrian evacuation efficiency, and can fit more than 90% of the changes. Specifically, except for index D ($P: 0.477/0.581$), which was insignificant in the two types

of CRD models, the rest were significant indices. The results showed that compared with network density, road width and road types, the influence of network connectivity on CRD pedestrian evacuation efficiency was not significant.

Table 8. Variance analysis of orthogonal test results.

	Mesh CRD ($R^2 = 0.900$)			Strip CRD ($R^2 = 0.943$)		
	F	p	Significance	F	p	Significance
Index A	8.792	0.010 **	√	7.488	0.015 *	√
Index B	5.352	0.033 *	√	9.86	0.007 **	√
Index C	6.325	0.023 *	√	15.22	0.002 **	√
Index D	0.814	0.477	×	0.581	0.581	×
Index E	23.71	0.001 **	√	56.933	0.000 **	√

* $p < 0.05$, ** $p < 0.01$.

3.2. Indices Importance Analysis

The importance analysis based on the range method was used to discuss the influence of each index under the synergistic effect. The test results of two CRD model types are shown in Table 9. Comparing the R value can measure the importance of each significant index: in strip type CRDs, A (R: 103.33) > E (R: 90.00) > B (R: 86.67) > C (R: 77.50); in mesh type CRDs, E (R: 127.22) > C (R: 115.00) > B (R: 95.00) > A (R: 81.67). The results showed that in the strip type CRDs, the road grade indices (A, E, B) have a more important impact on pedestrian evacuation efficiency than the network structure indices (C); while in the mesh type CRDs, the influence of network structure indices (C) was significantly improved.

Table 9. Range analysis of orthogonal test results.

	Strip CRD				Mesh CRD			
	Index A	Index B	Index C	Index E	Index A	Index B	Index C	Index E
K ₁	2940	2905	2755	3545	3585	3590	3645	4455
K ₂	2640	2385	2805	4355	3375	3020	3455	5600
K ₃	2320	2610	2340	-	3095	3445	2955	-
k ₁	490.00	484.17	459.17	393.89	597.50	598.33	607.50	495.00
k ₂	440.00	397.50	467.50	483.89	562.50	503.33	575.83	622.22
k ₃	386.67	435.00	390.00	-	515.83	574.17	492.50	-
R	103.33	86.67	77.50	90.00	81.67	95.00	115.00	127.22

3.3. Indices Optimal Level Analysis

The optimal level analysis based on the range method can be used to explore the correlation of various indices in the synergy and seek the optimal solution in the existing index level combination. Based on the visual diagram of the two CRD types' simulation test results (Figure 8), this research found that although there were differences in the influence degree, the action rules of each index were similar: the primary road width (A) was negatively correlated with the evacuation time, the wider the primary road, the higher the evacuation efficiency; the network density (C) was negatively correlated with the evacuation time, the denser the road network, the higher the evacuation efficiency, but there was no obvious difference in the effect on the medium and low density network of strip CRDs; the broken-line relationship between secondary road width (B) and evacuation time was optimal at a medium level, indicating that the secondary road width (B) should be appropriately set according to demand; the primary road type (E) affecting the proportion of pedestrian space was negatively correlated with evacuation time, indicating that the primary road with pedestrian traffic type had higher evacuation efficiency.

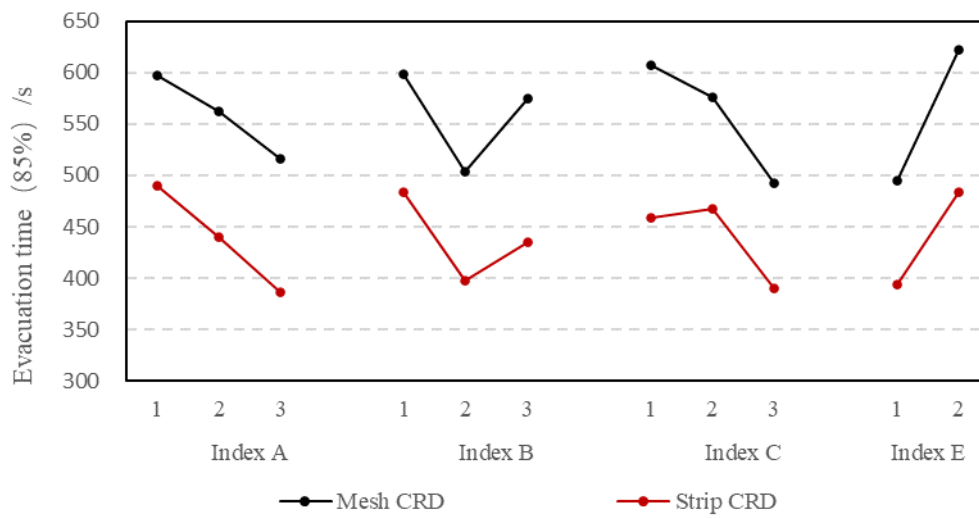


Figure 8. Visual diagram of range analysis results.

Since the longer the evacuation time, the lower the efficiency, the test results were negatively correlated with the optimal level of indices. Based on the three simulation schemes with the shortest evacuation time, we discerned the optimal level of multi-indices in two CRD types (Table 10). Among them, the optimal level combinations of strip CRD were: simulation scheme No.8 (A₃B₂C₃E₁, 285 s), No.5 (A₂B₂C₃E₁, 305 s) and No.7 (A₃B₁C₂E₁, 340 s); the optimal level combinations of mesh CRD were simulation scheme No.8 (A₃B₂C₃E₁, 370 s), No.5 (A₂B₂C₃E₁, 385 s) and No.2 (A₁B₂C₃E₁, 400 s). In general, the pedestrian primary road (E), “high density” network structure (B) and “medium width” secondary road (C) were beneficial to improve the pedestrian evacuation efficiency of the two CRD types. However, compared with the mesh CRD type, the strip CRD type had a higher demand for the primary road width (A).

Table 10. Indices optimal level arrangement based on ODOE.

CRD Type	Rank	Test ID	Evacuate Time	Model ID	Index A	Index B	Index C	Index E
Strip CRD	1	8	285 s	A ₃ B ₂ C ₃ E ₁	broad	medium	high	pedestrian
	2	5	305 s	A ₂ B ₂ C ₃ E ₁	medium	medium	high	pedestrian
	3	7	340 s	A ₃ B ₁ C ₂ E ₁	broad	medium	medium	pedestrian
Mesh CRD	1	8	370 s	A ₃ B ₂ C ₃ E ₁	broad	medium	high	pedestrian
	2	5	385 s	A ₂ B ₂ C ₃ E ₁	medium	medium	high	pedestrian
	3	2	400 s	A ₁ B ₂ C ₃ E ₁	broad	medium	high	pedestrian

4. Discussion

4.1. Parametric and Synergistic Effect Analysis

The ODOE study on the synergistic effect of road network planning indices on CRD pedestrian evacuation efficiency showed that there are differences in the analysis results of significance, importance and optimal level among the indices. Moreover, these differences were influenced by the CRD transportation and distribution (Table 11).

Table 11. Synergy of road network indices on pedestrian evacuation efficiency.

CRD Type	Strip CRD			Mesh CRD		
	Significance	Importance	Optimal Level	Significance	Importance	Optimal Level
Primary road width	✓	very important	30.1~40.0 m	✓	less important	30.1~40.0 m
Secondary road width	✓	medium	3.1~5.0 m/side	✓	medium	3.1~5.0 m/side
Network density	✓	less important	11.0~13.0 km/km ²	✓	important	11.0~13.0 km/km ²
Network connectivity	×	/	/	×	/	/
Primary road type	✓	important	pedestrian-traffic	✓	very important	pedestrian-traffic

In urban evacuation, network connectivity is an important planning indices that affects the evacuation efficiency of motor vehicles. Low road connectivity will cause traffic congestion [58,59]. This study found that the influence of network connectivity on CRD pedestrian evacuation efficiency was not significant using ODOE significance analysis. This discrepancy is due to the behavior difference between evacuees and motor vehicles. Evacuees are more mobile than motor vehicles, and can ignore the lane limit, turning radius, traffic signals and other control measures for motor vehicles [19,60,61]. Furthermore, due to the difference in volume size between people and motor vehicles, evacuees have relatively sufficient space at the urban level and can choose evacuation routes more freely.

This study found that the effects of network density, connectivity, road width and road type on CRD pedestrian evacuation efficiency are synergistic using ODOE importance analysis. Moreover, the synergistic effect of these road network planning indices is distinct in CRDs with different transportation and distribution. Leon et al. (2021) [20] analyzed the effect of network structure on pedestrian evacuation, but ignored the influence of road grade indices. Wang et al. (2020) [62] emphasized the influence of road width and type and thought that pedestrian roads were the best for pedestrian evacuation but did not consider the synergy of network structure indices. This study innovatively found the synergy of road network planning indices. Among strip CRDs, the road grade indices (primary road width, secondary road width and primary road type) have a more important influence on the pedestrian evacuation than the network structure indices (network density). However, the influence of the network structure indices (network density) in mesh CRDs is obviously improved.

Specifically, the primary road width and type have the highest influence on the pedestrian evacuation efficiency in the strip CRD. This is related to the CRD form and the distribution of people. The people in the strip CRD have the spatial characteristics of axial distribution along the primary road. The primary road area is limited, so it has high disaster sensitivity when the evacuees flood in. This results in the important influence of road width and road type on pedestrian evacuation efficiency (Figure 9). Meanwhile, the behavior tendency of nearby evacuation concentrates the evacuees on both sides of the primary road, which leads to primary road width (R: 103.33) being more important than primary road type (R: 90.00).

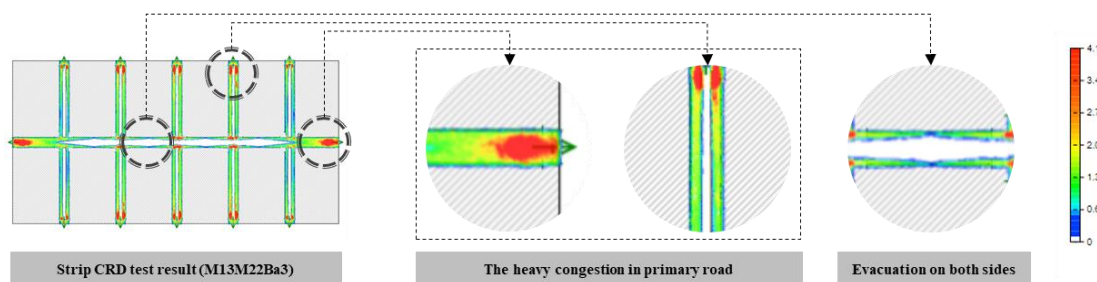


Figure 9. The congestion in pedestrian evacuation simulation of strip CRD.

The multi-axis intersection of transportation and distribution of mesh CRDs is relatively complicated. The centripetal distribution of people means the evacuees do not only concentrate on both sides of the primary road (Figure 10). The higher space occupancy rate strengthens the influence of road type on pedestrian evacuation efficiency, which leads to the result that primary road type (R: 127.22) is more important than primary road width (R: 81.67). The proportion of secondary roads is high, and the intersections are evenly distributed in mesh CRDs. The evacuation area and alternative evacuation routes can be obviously improved by increasing the number of secondary roads, which leads to the high importance of network density (R: 115.00).

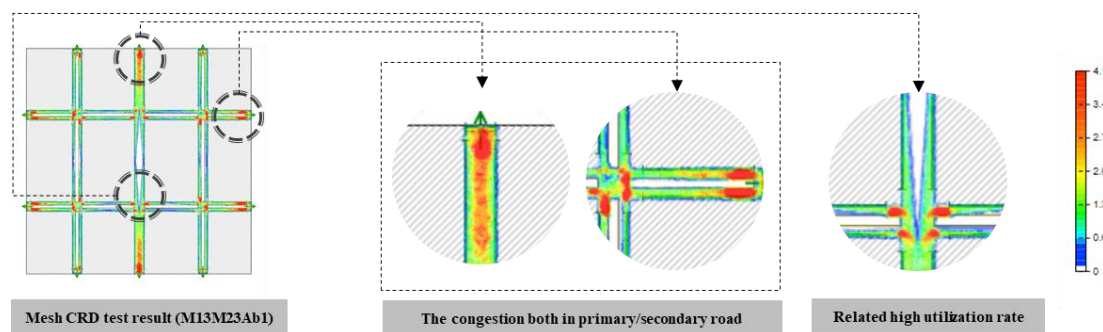


Figure 10. The congestion in pedestrian evacuation simulation of mesh CRD.

The suggested values of each road network planning indices under the synergy were found through ODOE optimal level analysis, which are similar in the two CRD types. Consistent with the existing research [17,63], the primary road width has the greatest pedestrian evacuation efficiency under broad width (30.1~40.0 m). However, the optimal level for secondary roads is medium width (pedestrian section of 3.1~5.0 m/side). This is because the medium width road provides sufficient distance for road intersections, which means the simulation agents can converge in a stable state, reducing the probability of congestion. The high-density network structure (11.0~13.0 km/km²) has the greatest pedestrian evacuation efficiency. Compared with motor vehicles [64,65], evacuees require higher network density because of their smaller body size.

4.2. Urban Design Implications

Based on the analysis results of synergy, aiming at improving the efficiency of pedestrian evacuation, the following CRD road network design suggestions are put forward from three aspects: block form, network structure and road grade.

1. Improving primary road grade

The primary road of a CRD should be a “broad width” pedestrian form according to the analysis results of optimal road grade level. A CRD primary road is the product of an urbanization process, which mainly shows two forms: walking and mixed-traffic commercial streets, according to different development stages [26]. Concessions at the bottom of building facades along the street and three-dimensional walking systems can establish continuous pedestrian roads, and ensure the primary road width is approximately 30.1~40.0 m.

2. Controlling secondary road width

The CRD secondary road width is suggested to be “medium width” according to the analysis results of optimal road grade level. When controlling the disorderly construction of secondary road width, methods such as intensive design of street facilities can be adopted to ensure the pedestrian space width is close to 3.1~5.0 m/side.

3. Increasing network density

The CRD road network is suggested to be “high density” according to the analysis results of optimal network structure level. CRD road networks have different densities due to diversified urban construction modes [66]. In low density CRDs, large-scale blocks can be broken by architectural design means, such as internal networks and partially overhead sections, to ensure a network density of 11.0~13.0 km/km².

4. Flexible road connection

The main and secondary roads are suggested to be flexibly connected according to the results of synergy significance analysis. Since the influence of network connectivity on pedestrian evacuation efficiency is not significant, non-ground facilities and temporary traffic control can be used to establish pedestrian branches, which can increase evacuation paths.

5. Ordered optimization

Different road network optimization orders are put forward for the two CRD types, according to the results of the importance analysis. It is more beneficial to improve the pedestrian evacuation efficiency of strip CRDs by improving the primary road grade first. However, increasing network density has a higher priority in mesh CRDs.

4.3. Limitations

Strip and mesh transportation and distribution are typical forms of CRD road network in China. This study is based on these two types. On a global scale, however, there are diversified CRD road network forms such as “radial” and “circular” [67]. The block form, network structure and road grade indices scale of these CRDs may have certain particularities. The above types can be further studied in the future.

The construction of CRD road networks has gradually entered the “three-dimensional” period. The traffic system uses non-ground facilities, which separates the people flow from the traffic flow and weakens the boundary of space. As pedestrian evacuation is more autonomous than motor vehicle, three-dimensional evacuation facilities separated from motor vehicle lanes have gradually attracted attention. However, the existing codes and research results still suggest evacuation with ground transportation facilities [7], which is also the direction that this study should continue to improve.

As for the method, ABM simulation technology was used to restore the pedestrian evacuation scene in this study. The Anylogic platform, based on the social force model, can well simulate the interaction between evacuees and the evacuation environment, but the behavior of agents at spatial nodes is still relatively rigid, and overlapping and vibrating errors occur. Using ORCA [68] and other models to modify and develop the ABM simulation platform could improve the authenticity and fluency of agents’ behavior in the environment and ensure the accuracy of research results.

The study results were obtained from simulation outcomes. These data is well applicable to the comparison between significance, importance and optimal level of different indices [22]. However, there are still some discrepancies with real-world situations in quantifying the evacuation efficiency under a specific index/level. This is caused by the incomprehensive restoration of real human behaviors by agents and is also a common problem of existing ABM platforms. Due to the social and ethical problems that threaten the safety of life and property in urban evacuation experiments, verification of the simulation results and real-world empirical data is limited. The parameters setting can be optimized through specific field interaction experiments in a further study to improve the authenticity of the simulation results.

5. Conclusions

With the trend of urban traffic construction returning to “human-based”, pedestrian evacuation has gradually become the focus of Safety City research. The Pedestrian Safety Action Plan formulated by the U.S. Department of Transportation (USDOT) points out that a reasonable and efficient road space environment is a requisite to ensure pedestrian evacuation efficiency. This study took the typical CRD road network forms in China as examples, and innovatively analyzed the synergy between road network planning indices and pedestrian evacuation efficiency. The road network planning indices included three aspects: block shape, network structure and road grade. The test variables were network density, network connectivity, road width and road type. The efficiency of pedestrian evacuation was measured by the completed evacuation time of 85% evacuees, as simulated in the Anylogic simulation platform. Additionally, the synergy analysis was completed using orthogonal DOE.

Through the analysis of significance, importance and optimal level, we have developed three research conclusions as follows. ① Compared with motor vehicle evacuation, the effect of network connectivity on pedestrian evacuation efficiency is not significant ($p > 0.4$ in the two types of CRD). ② The influence of road network density, road width and

road type on pedestrian evacuation efficiency is remarkable, but they shows different levels of importance in different CRD types. In mesh CRDs, the road level indices are relatively important. However, in strip CRDs, the importance of network structure indices are obviously improved. ③ The optimal level of road network planning indices in the two CRD types are similar. The network density should be controlled in the “high density” range of 10.1~13.0 km/km². The primary road should be set as a “broad width” pedestrian road with an effective evacuation width of 30.1~40.0 m. The effective evacuation width of secondary roads should be controlled in the “medium width” of 3.1~5.0 m. According to detailed research results, specific optimization methods and strategies are put forward for the primary/secondary road grade, network density, road connection and optimization order, which make it easier for urban designers to find a balance between improving pedestrian evacuation efficiency and building road networks.

Author Contributions: Conceptualization, Tiejun Zhou and Gen Yang; methodology, Gen Yang and Mingxi Peng; software, Dachuan Wang; validation, Gen Yang, Zhigang Wang and Dachuan Wang; formal analysis, Gen Yang; investigation, Gen Yang, Zhigang Wang and Mingxi Peng; writing—original draft preparation, Gen Yang; writing—review and editing, Gen Yang and Tiejun Zhou; visualization, Gen Yang; project administration, Tiejun Zhou; funding acquisition, Tiejun Zhou. All authors have read and agreed to the published version of the manuscript.

Funding: This research was funded by National Natural Science Foundation of China (NSFC), funding number 51678084 and 52278005.

Data Availability Statement: The data that support the findings of this study are available on request from the corresponding author.

Conflicts of Interest: The authors declare no conflict of interest.

References

1. United Nations Office for Disaster Risk Reduction. *GP2022 Co-Chairs' Summary*; United Nations Office for Disaster Risk Reduction: Bali, Indonesia, 2022.
2. UN-Habitat. *World Cities Report 2020—The Value of Sustainable Urbanization*; UN-Habitat: Nairobi, Kenya, 2020; Volume 51.
3. Amoako, C.; Cobbinah, P.B.; Nimminga-Beka, R. Urban Infrastructure Design and Pedestrian Safety in the Kumasi Central Business District, Ghana. *J. Transp. Saf. Secur.* **2014**, *6*, 235–256. [[CrossRef](#)]
4. Zeng, J.; Zuo, C. Analysis of disaster prevention and mitigation strategies in CBD spatial planning and design. *Archit. J.* **2010**, *11*, 75–79.
5. Ercolano, J.M. *Pedestrian Disaster Preparedness and Emergency Management: White Paper for Executive Management*; New York State Department of Transportation: Albany, NY, USA, 2007.
6. Zhou, T.J.; Wang, D.C. Discussion on the pedestrian emergency events evacuation preparedness space design of urban central areas: Literature review and research framework establishment. *Urban Archit.* **2017**, *21*, 21–26.
7. Zegeer, C.V.; Sandt, L.; Scully, M. *How to Develop a Pedestrian Safety Action Plan*; Federal Highway Administration: Chapel Hill, NC, USA, 2008; Volume 1.
8. Thomas, L.; Ryus, P.; Semler, C.; Thirsk, N.J.; Krizek, K.; Zegeer, C. Delivering safe, comfortable, and connected pedestrian and bicycle networks: A review of international practices. In *Pedestrian and Cyclist Safety: U.S. Trends and Initiatives and International Practices*; Nova Science Pub Inc.: Hauppauge, NY, USA, 2016.
9. Ercolano, J. Pedestrian disaster preparedness and emergency management of mass evacuations on foot: State-of-the-art and best practices. *J. Appl. Secur. Res.* **2008**, *3*, 389–405. [[CrossRef](#)]
10. Chen, P.; Zhang, J.; Zhang, L.; Sun, Y. Sun Evaluation of Resident Evacuations in Urban Rainstorm Waterlogging Disasters Based on Scenario Simulation: Daoli District (Harbin, China) as an Example. *Int. J. Environ. Res. Public Health* **2014**, *11*, 9964–9980. [[CrossRef](#)]
11. Nguyen, D.-T.; Shen, Z.-J.; Truong, M.-H.; Sugihara, K. Improvement of evacuation modeling by considering road blockade in the case of an earthquake: A case study of Daitoku school district, Kanazawa city, Japan. *Sustainability* **2021**, *13*, 2637. [[CrossRef](#)]
12. Xinhua News Agency. *The Number of Motor Vehicles in China Exceeded 400 Million*; Central People's Government of the People's Republic of China: Beijing, China, 2022.
13. Lee, J. A three-dimensional navigable data model to support emergency response in microspatial built-environments. *Ann. Assoc. Am. Geogr.* **2007**, *97*, 512–529. [[CrossRef](#)]
14. Dunn, C.E.; Newton, D. Optimal routes in GIS and emergency planning applications. *Area* **1992**, *24*, 259–267.
15. Yamada, T. A network flow approach to a city emergency evacuation planning. *Int. J. Syst. Sci.* **1996**, *27*, 931–936. [[CrossRef](#)]

16. Mohamadi, B.; Chen, S.; Liu, J. Evacuation priority method in tsunami hazard based on DMSP/OLS population mapping in the Pearl River estuary, China. *ISPRS Int. J. Geo-Inf.* **2019**, *8*, 137. [[CrossRef](#)]
17. Zhang, N.; Huang, H.; Su, B.; Zhao, J. Analysis of dynamic road risk for pedestrian evacuation. *Phys. A Stat. Mech. Its Appl.* **2015**, *430*, 171–183. [[CrossRef](#)]
18. Fang, Z.; Li, Q.; Li, Q.; Han, L.D.; Shaw, S.-L. A space-time efficiency model for optimizing intra-intersection vehicle-pedestrian evacuation movements. *Transp. Res. Part C Emerg. Technol.* **2013**, *31*, 112–130. [[CrossRef](#)]
19. Cova, T.J.; Johnson, J.P. A network flow model for lane-based evacuation routing. *Transp. Res. Part A Policy Pract.* **2003**, *37*, 579–604. [[CrossRef](#)]
20. León, J.; Vicuña, M.; Ogueda, A.; Guzmán, S.; Gubler, A.; Mokrani, C. From urban form analysis to metrics for enhancing tsunami evacuation: Lessons from twelve Chilean cities. *Int. J. Disaster Risk Reduct.* **2021**, *58*, 102215. [[CrossRef](#)]
21. Zhou, T.; Wang, D.; Zong, D.; He, X. The Study of the responsibility space regionalization of emergency shelters in the urban center and the evaluation of evacuation road based on microscope computer simulation—A Case of Chongqing Three Gorges Square Area. *Disaster Adv.* **2012**, *5*, 230–236.
22. Zuo, J.; Shi, J.; Li, C.; Mu, T.; Zeng, Y.; Dong, J. Simulation and optimization of pedestrian evacuation in high-density urban areas for effectiveness improvement. *Environ. Impact Assess. Rev.* **2020**, *87*, 106521. [[CrossRef](#)]
23. Shi, Z.; Hsieh, S.; Fonseca, J.A.; Schlueter, A. Street grids for efficient district cooling systems in high-density cities. *Sustain. Cities Soc.* **2020**, *60*, 102224. [[CrossRef](#)]
24. Minaei, M. Evolution, density and completeness of OpenStreetMap road networks in developing countries: The case of Iran. *Appl. Geogr.* **2020**, *119*, 102246. [[CrossRef](#)]
25. Jiang, F.; Ma, L.; Broyd, T.; Chen, K.; Luo, H.; Pei, Y. Sustainable road alignment planning in the built environment based on the MCDM-GIS method. *Sustain. Cities Soc.* **2022**, *87*, 104246. [[CrossRef](#)]
26. Shi, B.; Yang, J.; Zheng, Y. *The Centre of City: Urban Central Structure*; Springer: Singapore, 2021. [[CrossRef](#)]
27. Jin, J.G.; Shen, Y.; Hu, H.; Fan, Y.; Yu, M. Optimizing underground shelter location and mass pedestrian evacuation in urban community areas: A case study of Shanghai. *Transp. Res. Part A Policy Pract.* **2021**, *149*, 124–138. [[CrossRef](#)]
28. Irsyad, H.A.W.; Hitoshi, N. Flood disaster evacuation route choice in Indonesian urban riverbank kampong: Exploring the role of individual characteristics, path risk elements, and path network configuration. *Int. J. Disaster Risk Reduct.* **2022**, *81*, 103275. [[CrossRef](#)]
29. Wang, D.; Zhou, T.; Yang, G. Way-finding Strategies and Individual Influencing Factors of Fire Evacuation in Underground Commercial Buildings. In Proceedings of the 2019 9th International Conference on Fire Science and Fire Protection Engineering (ICFSFPE), Chengdu, China, 18–20 October 2019; pp. 1–6. [[CrossRef](#)]
30. Chen, D. The theory of the design of experiments. *Technometrics* **2001**, *43*, 497. [[CrossRef](#)]
31. Alsnihi, R.; Stopher, P.R. Review of the Procedures Associated with Devising Emergency Evacuation Plans. *Transp. Res. Rec.* **2004**, *1865*, 89–97. [[CrossRef](#)]
32. Chen, J.; Yu, J.; Wen, J.; Zhang, C.; Yin, Z.; Wu, J.; Yao, S. Pre-evacuation Time Estimation Based Emergency Evacuation Simulation in Urban Residential Communities. *Int. J. Environ. Res. Public Health* **2019**, *16*, 4599. [[CrossRef](#)]
33. Vermuyten, H.; Beliën, J.; De Boeck, L.; Reniers, G.; Wauters, T. A review of optimisation models for pedestrian evacuation and design problems. *Saf. Sci.* **2016**, *87*, 167–178. [[CrossRef](#)]
34. Hoppe, B.; Tardos, É. Quickest transshipment problem. *Math. Oper. Res.* **2000**, *25*, 36–62. [[CrossRef](#)]
35. Yu, J.; Zhang, C.; Wen, J.; Li, W.; Liu, R.; Xu, H. Integrating multi-agent evacuation simulation and multi-criteria evaluation for spatial allocation of urban emergency shelters. *Int. J. Geogr. Inf. Sci.* **2018**, *32*, 1884–1910. [[CrossRef](#)]
36. Yuksel, M.E. Agent-based evacuation modeling with multiple exits using NeuroEvolution of Augmenting Topologies. *Adv. Eng. Inform.* **2018**, *35*, 30–55. [[CrossRef](#)]
37. D’Orazio, M.; Spalazzi, L.; Quagliarini, E.; Bernardini, G. Agent-based model for earthquake pedestrians’ evacuation in urban outdoor scenarios: Behavioural patterns definition and evacuation paths choice. *Saf. Sci.* **2014**, *62*, 450–465. [[CrossRef](#)]
38. Shi, J.; Ren, A.; Chen, C. Agent-based evacuation model of large public buildings under fire conditions. *Autom. Constr.* **2009**, *18*, 338–347. [[CrossRef](#)]
39. Cheng, Z.; Lu, J.; Zhao, Y. Pedestrian Evacuation Risk Assessment of Subway Station under Large-Scale Sport Activity. *Int. J. Environ. Res. Public Health* **2020**, *17*, 3844. [[CrossRef](#)] [[PubMed](#)]
40. Boeing, G. OSMnx: New methods for acquiring, constructing, analyzing, and visualizing complex street networks. *Comput. Environ. Urban Syst.* **2017**, *65*, 126–139. [[CrossRef](#)]
41. Shi, Z.; Fonseca, J.A.; Schlueter, A. A parametric method using vernacular urban block typologies for investigating interactions between solar energy use and urban design. *Renew. Energy* **2020**, *165*, 823–841. [[CrossRef](#)]
42. Sharifi, A. Resilient urban forms: A review of literature on streets and street networks. *Build. Environ.* **2019**, *147*, 171–187. [[CrossRef](#)]
43. León, J.; March, A. Urban morphology as a tool for supporting tsunami rapid resilience: A case study of Talcahuano, Chile. *Habitat Int.* **2014**, *43*, 250–262. [[CrossRef](#)]
44. First-Tier City Research Institute. *China City Comprehensive Business Index Ranking in 2020*; China Business Network: Shanghai, China, 2020.
45. Ballard, D.H. Generalizing the Hough transform to detect arbitrary shapes. *Pattern Recognit.* **1981**, *13*, 111–122. [[CrossRef](#)]

46. Liu, B.; Shi, Y.; Li, D.-J.; Wang, Y.-D.; Fernandez, G.; Tsou, M.-H. An economic development evaluation based on the openstreetmap road network density: The case study of 85 cities in china. *ISPRS Int. J. Geo-Inf.* **2020**, *9*, 517. [[CrossRef](#)]
47. Lu, J.; Wang, W. Planning indices system of urban road network. *J. Traffic Transp. Eng.* **2004**, *4*, 62–67.
48. NACTO. *Global Street Design Guide*; Island Press: Washington, DC, USA, 2016.
49. Zurovac, J.; Brown, R. *Orthogonal Design: A Powerful Method for Comparative Effectiveness Research with Multiple Interventions*; Center on Healthcare Effectiveness: Washington, DC, USA, 2012.
50. Helbing, D.; Buzna, L.; Johansson, A.; Werner, T.; van Wageningen-Kessels, F.; Daamen, W.; Hoogendoorn, S.P.; Jiang, R.; Hu, M.-B.; Wu, Q.-S.; et al. Self-organized pedestrian crowd dynamics: Experiments, simulations, and design solutions. *Transp. Sci.* **2005**, *39*, 1–24. [[CrossRef](#)]
51. Borshchev, A.; Karpov, Y.; Kharitonov, V. Distributed simulation of hybrid systems with AnyLogic and HLA. *Future Gener. Comput. Syst.* **2002**, *18*, 829–839. [[CrossRef](#)]
52. Song, X.; Sun, J.; Xie, H.; Li, Q.; Wang, Z.; Han, D. Characteristic time based social force model improvement and exit assignment strategy for pedestrian evacuation. *Phys. A Stat. Mech. Its Appl.* **2018**, *505*, 530–548. [[CrossRef](#)]
53. Xu, H.; Tian, C.; Li, Y. Emergency evacuation simulation and optimization for a complex rail transit station: A perspective of promoting transportation safety. *J. Adv. Transp.* **2020**, *2020*, 8791503. [[CrossRef](#)]
54. Shatu, F.; Yigitcanlar, T.; Bunker, J. Shortest path distance vs. least directional change: Empirical testing of space syntax and geographic theories concerning pedestrian route choice behaviour. *J. Transp. Geogr.* **2019**, *74*, 37–52. [[CrossRef](#)]
55. Perry, R.W.; Lindell, M.K. Preparedness for emergency response: Guidelines for the emergency planning process. *Disasters* **2003**, *27*, 336–350. [[CrossRef](#)] [[PubMed](#)]
56. Wifipix. *Analysis of Customer Group Data of Typical Shopping Centers in Beijing and Shanghai*; Baidu: Beijing, China, 2016.
57. Lo, S.M.; Fang, Z.; Lin, P.; Zhi, G.S. An evacuation model: The SGEM package. *Fire Saf. J.* **2004**, *39*, 169–190. [[CrossRef](#)]
58. Ayo-Odifiri, O.S.; Fasakin, J.O.; Henshaw, F.O. Road Connectivity Approach to Eased Traffic Congestion on Market Roads in Benin Metropolis, Nigeria. *Am. J. Eng. Res.* **2017**, *6*, 41–48.
59. Dingil, A.E.; Rupi, F.; Stasiskiene, Z. A macroscopic analysis of transport networks: The influence of network design on urban transportation performance. *Int. J. Transp. Dev. Integr.* **2019**, *3*, 331–343. [[CrossRef](#)]
60. Savitha, B.G.; Murthy, R.S.; Jagadeesh, H.S.; Sathish, H.S.; Sundararajan, T. Study on Geometric Factors Influencing Saturation Flow Rate at Signalized Intersections under Heterogeneous Traffic Conditions. *J. Transp. Technol.* **2017**, *7*, 83–94. [[CrossRef](#)]
61. Kim, D.; Jeong, O. Cooperative traffic signal control with traffic flow prediction in multi-intersection. *Sensors* **2020**, *20*, 137. [[CrossRef](#)]
62. Wang, Z.; Zhou, T.; Yang, G. Study on the influence of effective width of roads in the central business district on the evacuation time in case of emergency. *Int. J. Electr. Eng. Educ.* **2020**. [[CrossRef](#)]
63. Usman, F.; Hariyani, S.; Shoimah, F. Perencanaan Partisipatif Tanggap Darurat Bencana Tsunami Di Pesisir Selatan Watulimo, Trenggalek. *TATALOKA* **2021**, *23*, 138–150. [[CrossRef](#)]
64. Wang, J.; Huang, H. Road network safety evaluation using Bayesian hierarchical joint model. *Accid. Anal. Prev.* **2016**, *90*, 152–158. [[CrossRef](#)]
65. Wang, X.; Yuan, J.; Schultz, G.G.; Fang, S. Investigating the safety impact of roadway network features of suburban arterials in Shanghai. *Accid. Anal. Prev.* **2018**, *113*, 137–148. [[CrossRef](#)] [[PubMed](#)]
66. Cai, J.; Cheng, M.; Zhu, F. Analysis of Impact of Key Indicators for Road Network Planning on Development Intensity: Case Study of 24 CBDs Worldwide. *Urban Plan. Forum* **2017**, *1*, 79–88.
67. Lynch, K. *Good City Form*; The MIT Press: Cambridge, MA, USA, 1984.
68. Berg, J.V.D.; Lin, M.; Manocha, D. Reciprocal velocity obstacles for real-time multi-agent navigation. In Proceedings of the 2008 IEEE International Conference on Robotics and Automation, Pasadena, CA, USA, 19–23 May 2008. [[CrossRef](#)]

Disclaimer/Publisher’s Note: The statements, opinions and data contained in all publications are solely those of the individual author(s) and contributor(s) and not of MDPI and/or the editor(s). MDPI and/or the editor(s) disclaim responsibility for any injury to people or property resulting from any ideas, methods, instructions or products referred to in the content.